ORGANOMETALLICS

Article

pubs.acs.org/Organometallics

Photo- and Thermal Isomerization of (TP)Fe(CO)Cl_2 [TP = Bis(2-diphenylphosphinophenyl)phenylphosphine]

Ping Li, Bas de Bruin, Joost N. H. Reek, and Wojciech I. Dzik*

Homogeneous, Supramolecular and Bio-Inspired Catalysis, van't Hoff Institute for Molecular Sciences, University of Amsterdam, Science Park 904, 1098 XH Amsterdam, The Netherlands

Supporting Information

ABSTRACT: The title complex displayed structural flexibility via photo- and thermal-isomerization reactions between three isomers: (*mer*-TP)Fe(CO)Cl_2 (**A**), *unsym*-(*fac*-TP)Fe(CO)-Cl_2 (**B**), and *sym*-(*fac*-TP)Fe(CO)Cl_2 (**C**). Irradiation of **A** at RT with 525 nm light selectively produces **B**, while at 0 °C isomer **C** is formed with the intermediacy of **B**. UV−vis spectroscopy combined with TD-DFT calculations revealed the nature of the photoisomerization process. Kinetics of the thermal isomerization of **C** to **B** and **B** to **A** have been studied with ^{31}P NMR spectroscopy in CD_2Cl_2, and activation parameters were determined. Isomers **A** and **B** have been isolated and crystallographically characterized.

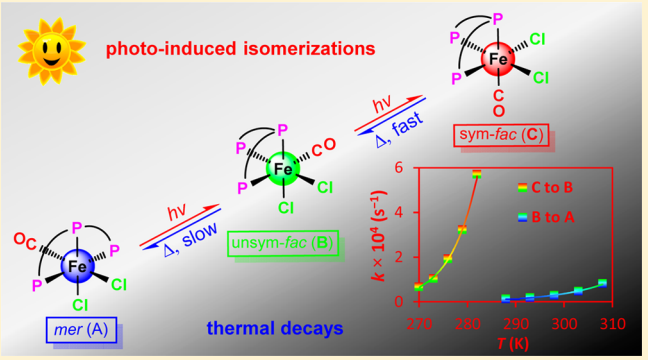

INTRODUCTION

The ability of molecules to change their shape upon external stimuli opens a variety of potential applications as molecular switches or machines.[1] In particular, the use of light as the switching factor has recently gained much interest in broad contexts spanning from biological applications to material science.[2]

In coordination chemistry, much attention has been focused on steering the properties of the transition metal by switching the conformation of a photoactive substituent appended to the ligand. In this way properties such as spin state of the metal can be tuned.[3] The opposite situation in which the photoevent within the coordination sphere of the metal dictates the conformational change of the ligand is much less common. Examples are the reversible phototriggered change of denticity of polyamine ligands accompanied by (de)coordination of an auxiliary ligand[4] and *mer-fac*-isomerization of octahedral complexes with tridentate ligands.[5] In the latter case the denticity of the isomerized ligand does not change; that is, there is no net formation or breaking of bonds, which can be beneficial when rigidity of photoswitches is desired. It is noteworthy that so far all the examples of photochemical metal-dictated conformational change of the ligand proceeded on noble metal centers. As such, the discovery of base-metal complexes that reveal such behavior would enable the development of a new class of low-cost photoswitches.

In the context of our studies on photochemical proton reduction,[6,7] we discovered that the iron complex (TP)Fe-(CO)Cl_2 (TP = bis[2-(diphenylphosphino)phenyl]-phenylphosphine) undergoes light-induced isomerization from the *mer*- to *fac*-coordination mode of the tridentate TP ligand, followed by a slow thermal reisomerization. Here, we report the synthesis and structural characterization of the title complex, photoisomerization, and kinetic studies of the thermal-isomerization reactions.

RESULTS AND DISCUSSION

Synthesis and Characterization of (TP)Fe(CO)Cl_2 Complexes. (*mer*-TP)Fe(CO)Cl_2 (**A**) was synthesized in 92% yield by treating $FeCl_2 \cdot 4H_2O$ with a stoichiometric amount of TP in a mixture of CH_2Cl_2 and MeOH under an atmosphere of carbon monoxide in the dark. Spectroscopic analysis of **A** revealed the presence of a single carbonyl ligand, as evidenced by the IR absorption band at 1972 cm^{-1}, and a C_s symmetric orientation of the TP ligand evidenced by two ^{31}P NMR resonances in CD_2Cl_2: a triplet at 115.64 ($^2J_{PP}$ = 32.4 Hz) and a doublet at 65.11 ppm ($^2J_{PP}$ = 32.4 Hz), with an integral ratio of 1:2.

When a solution of **A** in CH_2Cl_2 was brought into ambient light, a slow color change from orange to dark red was observed. This is accompanied by changes in the ^{31}P NMR spectrum, which displayed a set of three resonances: a doublet of doublets at 111.55 ($^2J_{PP}$ = 32.4 Hz, $^2J_{PP}$ = 47.0 Hz); a doublet of doublets at 77.60 ($^2J_{PP}$ = 32.0 Hz, $^2J_{PP}$ = 47.0 Hz); and a triplet at 53.60 ppm ($^2J_{PP}$ = 47.0 Hz), with an integral ratio of 1:1:1. The spectrum represents the formation of new species **B** with a C_1 symmetry indicative of an *unsym*-(*fac*-TP)Fe(CO)Cl_2 structure. The IR carbonyl stretch of 2008 cm^{-1} is indicative of weakening of π-back-donation from the iron center.

Received: July 9, 2015

DOI: 10.1021/acs.organomet.5b00644
Organometallics XXXX, XXX, XXX−XXX

Solid-state structures of species **A** and **B** were obtained by single-crystal X-ray diffraction (Figure 1). In both structures,

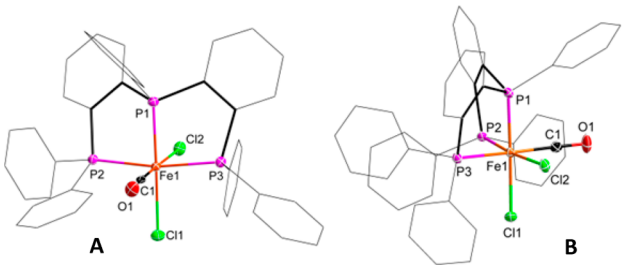

Figure 1. X-ray structures of isomers **A** (left) and **B** (right). Hydrogen atoms and cocrystallized CH_2Cl_2 solvent molecules are omitted for clarity. Selected bond lengths (Å) and angles (deg) for **A**: Fe1−P1 2.1852(10), Fe1−P2 2.2547(9), Fe1−P3 2.2422(9), Fe1−Cl1 2.3410(10), Fe1−Cl2 2.3523(9), Fe1−C1 1.743(4), C1−O1 1.141(4); P1−Fe1−P2 84.15(4), P1−Fe1−P3 86.49(4), P2−Fe1−P3 169.17(4). For **B**: Fe1−P1 2.1639(6), Fe1−P2 2.2212(6), Fe1−P3 2.3369(6), Fe1−Cl1 2.3308(6), Fe1−Cl2 2.3499(6), Fe1−C1 1.790(2), C1−O1 1.139(3); P1−Fe1−P2 88.13(2) P1−Fe1−P3 83.91(2) P2−Fe1−P3 101.08(2).

each iron center is coordinated to a TP ligand, one carbonyl ligand, and two chlorides and adopts a slightly distorted octahedral configuration. The TP ligand coordinates to the Fe center in a meridional fashion in isomer **A** and a facial fashion in isomer **B**. The meridional coordination mode of the TP ligand in **A** is remarkable, as none of the previously reported mononuclear complexes of TP reveal such a binding mode.[8] As such, isomer **A** is the first metal complex that features TP as a PPP pincer-type ligand.[9] This behavior is, however, in accord with the expected binding mode of three phosphine donors to an octahedral monocarbonyl iron(II) species.[10] The two terminal phosphorus atoms P2 and P3 in isomer **A** (Figure 1) are *trans* to each other with similar bond distances to the iron center (2.2547(9) Å for Fe1−P2 and 2.2422(9) Å for Fe1−P3), while the Fe1−P1 bond distance 2.1852(10) Å) is significantly shorter. In contrast, the bond distance for Fe1−P3 (2.3369(6) Å) in isomer **B** is significantly longer than that for Fe1−P2 (2.2212(6) Å) due to the stronger *trans* influence of the carbonyl ligand compared to the chloride.

When a solution of **B** in CH_2Cl_2 was kept in the dark, isomer **A** was fully recovered within 2 days, as indicated by ^{31}P NMR. The isomerization of **B** to **A** in CH_2Cl_2 was also monitored using IR and UV−vis spectroscopy, as shown in Figure 2. The stretching frequency of the carbonyl ν(CO) displayed a red shift from 2008 cm^{-1} in **B** to 1972 cm^{-1} in **A**. This observation is consistent with the single-crystal structures showing significantly shorter bond distance of Fe−C1 (*trans* to a π-donating chloride) in isomer **A** (1.743(4) Å) than that in

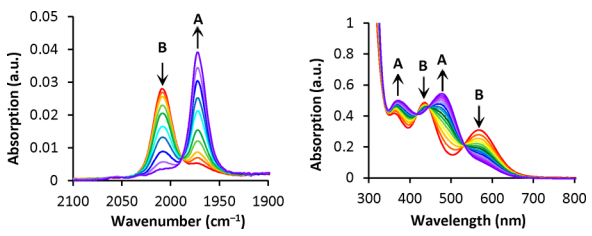

Figure 2. IR (left) and UV−vis (right) spectral change during the thermal isomerization of **B** to **A** in CH_2Cl_2 in the dark at 298 K.

isomer **B** (1.790(2) Å), reflecting stronger back-donating ability from Fe to CO in isomer **A**. The UV−vis spectra displayed three clear isosbestic points at 419, 447, and 532 nm. The intense visible absorption shifted from 566 nm in **B** to 482 nm in **A**, which is in agreement with the color change from dark red to orange.

The ability of iron(II) carbonyl compounds to undergo photochemical isomerization followed by thermal rearrangement to the initial state is well established.[11] Depending on the wavelength the photorearrangement can proceed via either CO loss or halide dissociation,[12] and in principle both pathways could also be operational during the isomerization of **A** to **B** triggered by visible light. The UV−vis spectrum of **A** reveals two separate bands with peak maxima at λ = 366 and 482 nm. In most cases, the lowest (singlet) excited state is most relevant to explain the photoreactivity of a compound, and indeed selective irradiation of the lowest energy band of **A** using a 525 nm LED lamp leads to clean formation of **B** in CD_2Cl_2 with a quantum yield of Φ = 0.72.[13]

TD-DFT calculations reveal that the 482 nm band of **A** (484 nm in DFT) is a mixed excitation consisting of HOMO → LUMO and HOMO → LUMO+1 transitions. Excitation of this band is associated with a Fe−Cl → TP-ligand charge transfer process, with a small contribution of Fe in the two acceptor orbitals (see the SI). Since the HOMO of **A** is essentially an Fe−Cl π*-antibonding orbital, the photochemical reaction of **A** to **B** mostly seems to involve photodissociation of a chlorine atom. Complex **B** can only be selectively converted back to **A** thermally. Attempts to convert **B** back to **A** in a photochemical reaction were only partly successful. When the 566 nm band of **B** was irradiated with 590 nm LED light, a steady-state mixture of **A** and **B** was obtained (presumably due to overlap of the bands of **A** and **B**).

Kinetic Studies. To get insight on the thermal back-isomerization of **B** to **A**, we conducted kinetic measurements using variable-temperature ^{31}P NMR spectroscopy (Figure 3).

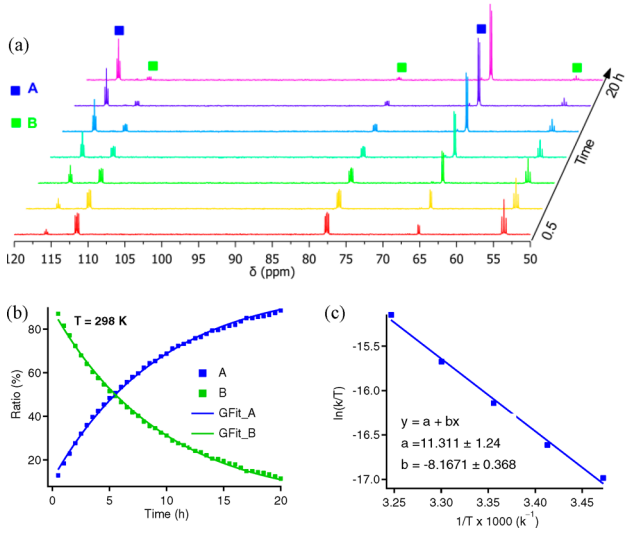

Figure 3. Thermal isomerization of **B** to **A** in CD_2Cl_2 in the dark. (a) $^{31}P\{^1H\}$ NMR spectra at 298 K. (b) Kinetic curves obtained from $^{31}P\{^1H\}$ NMR integrations for **B** (green) and **A** (blue) at 298 K. k = (2.91 ± 0.02) × 10^{-5} s^{-1}. (c) Eyring plot of the thermal isomerization of **B** to **A**: $\Delta H^{\ddagger}$ = 16.23 ± 0.73 kcal mol^{-1}, $\Delta S^{\ddagger}$ = −24.74 ± 2.70 cal mol^{-1} K^{-1}, $\Delta G^{\ddagger}$(298 K) = 23.60 kcal mol^{-1}.

DOI: 10.1021/acs.organomet.5b00644
Organometallics XXXX, XXX, XXX−XXX

Over the period of of 20 h, the conversion of **B** to **A** reached more than 90% in CD_2Cl_2 at 298 K. The kinetic profile in Figure 2b could be fitted with a first-order reaction ($d[B]/dt = -k[B]$), giving the reaction rate constant $k = (2.91 \pm 0.02) \times 10^{-5}$ s^{-1}. The reaction rate constant for isomerization of **B** to **A** was measured at various temperatures in the range between 288 and 308 K (Scheme S1 and Figures S8–S12). Plotting $\ln(k/T)$ as a function of $1/T$ gave a linear Eyring profile (Figure 3c). The linear fitting parameters afforded the activation parameters for the thermal isomerization of **B** to **A** in CD_2Cl_2 as $\Delta H^{\ddagger} = 16.23 \pm 0.73$ kcal mol^{-1}, $\Delta S^{\ddagger} = -24.74 \pm 2.70$ cal mol^{-1} K^{-1}, and $\Delta G^{\ddagger}(298\ K) = 23.60$ kcal mol^{-1}.

Interestingly, when irradiation of **A** was conducted at 0 °C, a third species in addition to isomers **A** and **B** was detected. IR spectroscopy revealed a monocarbonyl species with $\nu CO = 1988$ cm^{-1} (Figure S1). The $^{31}P\{^1H\}$ spectrum of this species (bottom curve in Figure 4a) displayed a triplet at 108.07 ppm

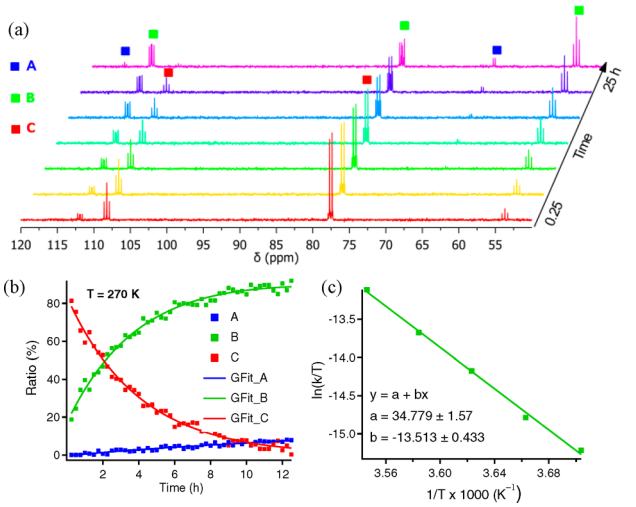

Figure 4. Thermal isomerization of **C** to **B** in CD_2Cl_2 in the dark. (a) $^{31}P\{^1H\}$ NMR spectra at 270 K. (b) Kinetic curves obtained from $^{31}P\{^1H\}$ NMR integrations for isomers **C** (red), **B** (green), and **A** (blue) at 270 K. (c) Eyring plot of the isomerization of **C** to **B**: $\Delta H^{\ddagger} = 26.85 \pm 0.86$ kcal mol^{-1}, $\Delta S^{\ddagger} = 21.90 \pm 0.99$ cal mol^{-1} K^{-1}, $\Delta G^{\ddagger}(270\ K) = 20.94$ kcal mol^{-1}.

($^2J_{PP} = 43.7$ Hz) and a doublet at 77.41 ppm ($^2J_{PP} = 43.7$ Hz) with the integral ratio of 1:2, indicating a C_s symmetric environment of iron. Three of such isomers can be considered: *fac*-complex **C** in which the chlorides are *trans* to the P2 and P3 donors and the carbonyl ligand is *trans* to the P1 donor; a *mer*-complex **D** in which the carbonyl ligand is *trans* to the P1 donor; and a *mer*-complex **E**, which is the conformational isomer of **A** in which the phenyl ring is pointing toward the chloride instead of the carbonyl (Figure 5). For a *mer*-coordination mode of the species formed at low temperature one would expect the ^{31}P chemical shift of phosphines P2 and P3 to be close to 65 ppm as it is in **A**. The value of 77.41 suggests that both phosphines are coordinated *trans* to chlorides, thus rendering isomer **C** the most plausible structure for this intermediate. Unfortunately, all attempts to crystallize this species under irradiation failed, preventing us from establishing the structure of **C** in the solid state. DFT (BP86/def2-TZVP) was used to calculate the relative energies of all the possible octahedral isomers of $(TP)Fe(CO)Cl_2$ (**A**–**E**, Figure 5). In agreement with the experiment, the dark

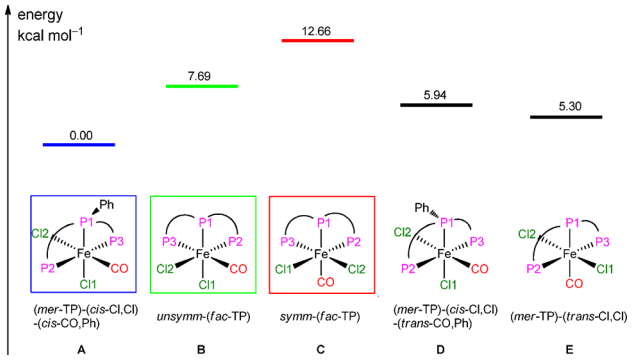

Figure 5. DFT (BP86/def2-TZVP)-calculated energy levels for all possible octahedral isomers of $(TP)Fe(CO)Cl_2$.

isomer **A** has the lowest energy. Isomer **B** is 6.7 kcal/mol higher in energy. The configuration of *sym*-(*fac*-TP)$Fe(CO)Cl_2$ (**C**) that was proposed as the species formed at 0 °C has higher (5 kcal mol^{-1}) energy than isomer **B**, which is consistent with the thermal decay of **C** to **B** in solution, as discussed below.[14] Species **D** and **E** are both calculated to be higher in energy than species **B** and are thus not expected to re-form thermally to **B**. The assignment of isomer **C** was also supported by the DFT-calculated IR spectra. In accord with the experiments, the carbonyl stretching frequency of structure **C** lies in between the values of **A** and **B** (Figure 5 and Table S3). The TD-DFT-calculated UV–vis spectrum of **C** reveals only a weak absorption in the visible region, in accordance with the experimental spectrum (one main band at 366 nm; see the SI).

The $^{31}P\{^1H\}$ NMR spectra shown in Figure 4a display the spectral changes during the decay of **C** in solution in the dark at 270 K. The isomerization reaction of **C** to **B** was accompanied by the formation of some **A**. The global fit (Scheme S2 and equations S3–5) of the reaction profile in Figure 4b suggested that the decay of **C** afforded only **B**, while a small amount of **A** was formed by subsequent thermal decay of **B**. Activation parameters for the isomerization of **C** to **B** were obtained from the Eyring plot (Figure 4b) as $\Delta H^{\ddagger} = 26.85 \pm 0.86$ kcal mol^{-1}, $\Delta S^{\ddagger} = 21.90 \pm 0.99$ cal mol^{-1} K^{-1}, and $\Delta G^{\ddagger}(270\ K) = 20.94$ kcal mol^{-1}. The decay of **C** to **B** is much faster than the decay of **B** to **A** at the same temperature (Figure 6). The half-life

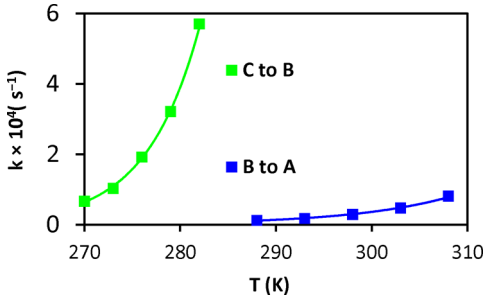

Figure 6. Reaction rate constant of thermal isomerization reactions of **C** to **B** and **B** to **A** in CD_2Cl_2 measured by ^{31}P NMR.

($\tau_{1/2}$) of photoproduct **C** can be extended from 90 s at 298 K to 1.74 h at 273 K (Figure S18), which enabled us to study the photoisomerization process in a relatively short time with little interference from the decay of **C** to **B** (Figure S19). Following the irradiation at 273 K in time with ^{31}P NMR revealed full conversion of **A** to a mixture of **B** and **C** within 3 min, followed

DOI: 10.1021/acs.organomet.5b00644
Organometallics XXXX, XXX, XXX–XXX

by full conversion of residual **B** to **C** within the next 7 min. Isomer **B** can thus be regarded as a structural intermediate during both the light-induced isomerization of **A** to **C** and also the backward decay from **C** to **A**, as shown in Scheme 1.

Scheme 1. Stepwise Photo- and Thermal Isomerization Reactions

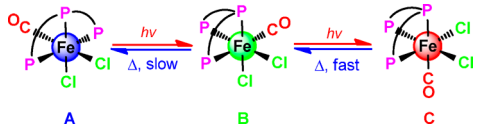

Mechanistic Considerations. As discussed above, based on TD-DFT calculations the proposed photoisomerization mechanism involved photoinduced dissociation of a chlorine atom, followed by TP ligand rearrangement and recapture of the chlorine atom. In regard to the mechanisms of the thermal isomerization reactions, the dissociation of one of the coordinating groups (P, Cl, or CO) might be the initial step before the rearrangement of the geometry around the iron center.[15] Thermal decay from **B** to **A** is significantly slowed down in the presence of 1 atm of CO, which had little effect on the isomerization from **C** to **B** (see the SI, Figures S20 and S21, respectively). Carbonyl dissociation could thus be proposed as the initial step for the thermal isomerization of **B** to **A** but not for **C** to **B**. However, the highly negative entropy of activation for the thermal isomerization of **B** to **A** is not in accord with a dissociative process of an L-type ligand. A similar negative entropy of activation value has been reported for *mer*-to-*fac* isomerization of $MnBr(CO)_3(bpy')$ in THF (bpy′ = 4,4′-dimethyl-2,2′-bipyridine), and an ionic mechanism (halide dissociation) was proposed.[16] In that case the decrease of entropy would be caused by electrostriction of the solvent resulting from formation of charged species. This appears to be the case here as well. Addition of methanol, which can stabilize the dissociated Cl^- ion to the freshly prepared solution of **B** in DCM, led to instant disappearance of the ^{31}P signals of **B**, accompanied by clean formation of **A** within 1 h.[17]

We used DFT to investigate whether the initial dissociation of the chlorido ligand from **B** could lead to the formation of species **A**. On the singlet surface, dissociation of a chlorido ligand leads to the formation of a square pyramidal species $^1\mathbf{B}^+(\text{-}\mathbf{Cl}^-)$, in which CO and the remaining chlorido ligand are coordinated in the basal positions. This species easily isomerizes over a transition state that has an energy 2.6 kcal/mol higher than $^1\mathbf{B}^+(\text{-}\mathbf{Cl}^-)$ to a lower energy (ΔE_{SCF} = −1.5 kcal/mol) square pyramidal $^1\mathbf{A}^+(\text{-}\mathbf{Cl}^-)$ species with the CO ligand coordinated at the apical position. Recoordination of the chlorido ligand to the latter species would lead to the formation of species **A**. Remarkably, on the triplet surface, only $^3\mathbf{A}^+(\text{-}\mathbf{Cl}^-)$ could be located as a minimum (ΔE_{SCF} = +1.2 kcal/mol vs $^1\mathbf{B}^+(\text{-}\mathbf{Cl}^-)$). These calculations show that dissociation of a chloride from **B** should lead to facile formation of **A** regardless of the spin state of the putative five-coordinate intermediate (Scheme 2), which is in accord with the observed acceleration of isomerization in the presence of methanol.

The positive activation entropy of the thermal isomerization of **C** to **B** points to a transition state with a dissociated phosphine arm. The thus formed high-spin pentacoordinate intermediate could subsequently isomerize, for example, via a Berry-pseudorotation pathway and yield **B** after recoordination of the phosphine arm. Quantum chemical modeling of possible dissociative thermal-isomerization pathways would require a detailed treatment of both singlet and triplet surfaces, which is beyond the scope of this study.

Scheme 2. Thermal Isomerization of B to A Proceeding via Chloride Dissociation

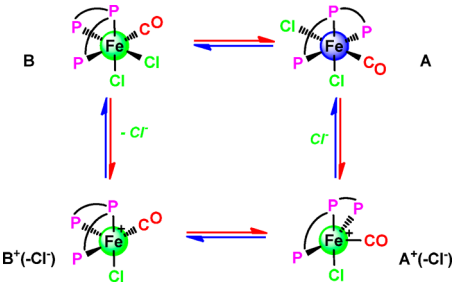

CONCLUSION

In conclusion, we show that a tridentate phosphine ligand coordinated to an iron(II) carbonyl center can undergo photoinduced *mer*- to *fac*-isomerization with the reverse process occurring thermally. This is a rare example of a photoswitch operating via the change of geometry of a coordinated ligand triggered by a photoevent within the coordination sphere of a first-row transition metal.

EXPERIMENTAL SECTION

General Considerations. All experiments and manipulations were carried out under a dry and oxygen-free atmosphere of nitrogen or argon using standard Schlenk techniques unless otherwise specified. Solvents were dried and distilled over an appropriate drying agent under an atmosphere of nitrogen. All commercially available reagents were used as received. Bis(2-diphenylphosphinophenyl)-phenylphosphine][8a] was prepared according to a modified procedure based on a literature report. The ^1H, ^{13}C, and ^{31}P NMR spectra were collected with a Varian Mercury 300 MHz or Bruker AVANCE 400 MHz spectrometer. Infrared spectra were recorded with a Nicolet Nexus FT-IR spectrometer. UV−vis absorption spectra were recorded with an HP G1103A spectrometer. *trans*-4-(Dicyanomethylene)-2-methyl-6-(4-dimethylaminostyryl)-4*H*-pyran was used as a reference to determine the quantum yield.[18] High-resolution mass spectra (HRMS) were recorded with an AccuTOF GC v 4g, JMS-T100GCV mass spectrometer. Elemental analyses were performed by Mikroanalytisches Labor Kolbe, Mülheim, Germany.

Synthesis of Bis[2-(diphenylphosphino)phenyl]-phenylphosphine]. To a solution of (2-bromophenyl)-diphenylphosphine (2.60 g, 7.62 mmol) in ether (30 mL) cooled at −40 °C was added dropwise a solution of *n*BuLi (1.6 M in hexane, 5 mL, 8.0 mmol) under stirring. The cold solution was stirred for 10 min at −40 °C and anther 2 h from −40 °C to room temperature. A solution of $PhPCl_2$ (682 mg, 3.81 mmol) in ether (10 mL) was added dropwise under stirring. After being stirred overnight at room temperature, the solution was filtered. The thus-obtained white solid was washed with ether (10 mL × 2) and dried in vacuo. The white powder was extracted with CH_2Cl_2 (60 mL × 3). The crude product was obtained by solvent evaporation under reduced pressure. Analytically pure product was obtained after flash column chromatography on silica gel (60−200 μm) using a mixture of CH_2Cl_2 and hexane (1:1, v/v) as eluent. Yield: 0.86 g, 36%. ^1H NMR (400 MHz, CD_2Cl_2, 298 K): δ 7.26−6.86 (m, 33H) ppm. ^{31}P (162 MHz, CD_2Cl_2, 298 K): δ 14.87 (d[AB] $^2J_{PP}$ = 175 Hz, 1P), 14.95 (d[AB] $^2J_{PP}$ = 125 Hz, 1P), 17.89 (dd[AB] $^2J_{PP}$ = 175 Hz, $^2J_{PP}$ = 123 Hz, 1P) ppm. ^{13}C NMR (101 MHz, CD_2Cl_2, 298 K): δ 137.57 (s), 137.45 (s), 137.34 (s), 137.12 (m), 134.30 (s), 134.24 (s), 134.18 (s), 134.12 (s), 134.04 (s), 133.64 (s), 133.54 (s), 133.44 (s), 133.34 (s), 128.89 (s), 128.60

DOI: 10.1021/acs.organomet.5b00644
Organometallics XXXX, XXX, XXX−XXX

(s), 128.07 (m) ppm. Anal. Calcd ($C_{42}H_{33}P_3$): C, 79.99; H, 5.27. Found: C, 80.07; H, 5.23

Synthesis of (mer-TP)Fe(CO)Cl$_2$ (A). Under an atmosphere of carbon monoxide, a solution of TP (473 mg, 0.75 mmol) in CH_2Cl_2 (30 mL) was added to a solution of $FeCl_2{\cdot}2H_2O$ (150 mg 0.75 mmol) in MeOH (5 mL) under stirring at room temperature. A red solution was formed immediately and turned to bright red after being stirred for another 30 min in the dark under an atmosphere of carbon monoxide. Solvent was removed under reduced pressure, and the resulting orange powder was washed with MeOH (10 mL × 2) and ether (10 mL × 2), respectively. The isomer **A**·$1.2CH_2Cl_2$ was isolated as an orange powder. Yield: 540 mg (0.61 mmol, 81%). Single crystals suitable for X-ray diffraction were grown as orange needles by the diffusion of THF to a solution of **A** in CH_2Cl_2 in the dark at room temperature. ^{1}H NMR (400 MHz, CD_2Cl_2, 298 K): δ 8.28 (t, J = 7.2 Hz, 2H), 7.94 (m, 4H), 7.83 (m, 2H), 7.73 (m, 4H), 7.66 (m, 4H), 7.44 (m, 3H), 7.36 (m, 8H), 7.03 (t, J = 7.2 Hz, 2H) 6.82 (dt, J = 2.4 Hz, J = 7.2 Hz, 2H) 6.39 (m, 2H) ppm. ^{13}C (101 MHz, CD_2Cl_2, 298 K): δ 136.62 (t, J = 4.44 Hz) 135.88 (s), 135.73 (s), 133.05 (t, J = 5.15 Hz), 132.42 (t, J = 6.16) 131.76 (s), 131.65 (s), 131.40 (m), 130.60 (s), 130.53 (s), 128.55 (t, 4.44 Hz), 128.33 (s), 128.23 (s), 127.75 (t, J = 4.80) ppm. ^{31}P (162 MHz, CD_2Cl_2, 298 K): δ 115.64 (t, $^2J_{PP}$ = 32.4, 1P), 65.11 (d, $^2J_{PP}$ = 32.4 Hz, 2P) ppm. IR (CH_2Cl_2, cm^{-1}): ν(C≡O) 1972 (s). HRMS (FD+) m/z: $[M - CO]^+$ calcd for $C_{42}H_{33}Cl_2Fe_1P_3$ 756.05216, found 756.05831. Anal. Calcd ($C_{43}H_{33}Cl_2FeOP_3{\cdot}1.2CH_2Cl_2$): C, 59.83; H, 4.02. Found: C, 59.83; H, 4.14

Synthesis of unsym-(fac-TP)Fe(CO)Cl$_2$ (B). A Schlenk tube containing a solution of (*mer*-TP)Fe(CO)Cl_2 (**A**)·$1.2CH_2Cl_2$ (50 mg, 0.056 mmol) in CH_2Cl_2 (4 mL) was placed in a fume hood with the light on. The color of the solution changed from bright to dark red in several hours. Single crystals suitable for X-ray diffraction were collected after the slow evaporation of solvent as the isomer **B**·$0.5CH_2Cl_2$. Yield: 43 mg (0.052 mmol, 93%). ^{1}H NMR (400 MHz, CD_2Cl_2, 298 K): δ 8.14 (t, J = 8.5 Hz, 2H), 7.91 (dt, J = 15.7, 7.5 Hz, 2H), 7.69−7.61 (m, 3H), 7.60−7.51 (m, 4H), 7.50−7.37 (m, 10H), 7.33 (d, J = 9.1 Hz, 4H), 7.22−7.16 (m, 1H), 6.99 (t, J = 7.3 Hz, 2H), 6.89 (t, J = 7.5 Hz, 1H), 6.57 (t, J = 7.6 Hz, 2H), 6.46 (t, J = 8.6 Hz, 2H). ^{13}C NMR (101 MHz, CD_2Cl_2, 223 K): δ 134.33 (d, J = 8.48 Hz), 131.64 (s), 131.54 (s), 130.92 (s), 130.27 (s), 130.18 (s), 130.06 (s), 129.71 (s), 129.59 (s), 129.32 (s), 128.24 (s), 128.14 (s), 128.05 (s), 127.65 (s), 127.53 (s), 127.44 (s), 127.22 (s), 127.14 (s), 126.63 (s), 126.53 ppm (s). ^{31}P (162 MHz, CD_2Cl_2, 298 K): δ 111.55 (dd, $^2J_{PP}$ = 32.4 Hz, $^2J_{PP}$ = 47.0 Hz, 1P), 77.60 (dd, $^2J_{PP}$ = 32.4 Hz, $^2J_{PP}$ = 47.0 Hz, 1P), 53.60 (t, $^2J_{PP}$ = 47.0 Hz, 1P) ppm. IR (CH_2Cl_2, cm^{-1}): ν(C≡O) 2008 (s). HRMS (FD+) m/z: $[M - CO]^+$ calcd for $C_{42}H_{33}Cl_2Fe_1P_3$ 756.05216, found 756.06375. Anal. Calcd ($C_{43}H_{33}Cl_2FeOP_3{\cdot}0.5CH_2Cl_2$): C, 63.11; H, 4.14. Found: C, 63.34; H, 4.55. Note: Absolutely pure NMR spectra of isomer **B** are not available due to its decay to isomer **A**. The ^{13}C NMR spectrum was recorded at −50 °C to slow down the decay process.

Photogeneration of sym-(fac-TP)Fe(CO)Cl$_2$ (C). An NMR tube containing a solution of isomer (*mer*-TP)Fe(CO)Cl_2 (**A**) in CD_2Cl_2 was placed in a cooling bath at 0 °C. After being irradiated by a 120 W halogen lamp for 30 min, the NMR tube was transferred to a −78 °C cold bath before it was measured in an NMR spectrometer. A full conversion to isomer **C** could not be reached, as evidenced by ^{31}P{^{1}H} NMR, as **C** always decayed to both **B** and **A**, as discussed in the main text. ^{31}P NMR (162 MHz, CD_2Cl_2, 276 K): δ 108.07 (t, $^2J_{PP}$ = 43.7 Hz, 1P), 77.41 (d, $^2J_{PP}$ = 43.9 Hz, 2P) ppm. IR (CH_2Cl_2, cm^{-1}): ν(C≡O) 1988 (s).

X-ray Single-Crystal Determination. Data were collected on a Bruker D8 Quest Eco diffractometer, equipped with a TRIUMPH monochromator and a CMOS PHOTON 50 detector, using Mo Kα radiation (λ = 0.710 73 Å). All experiments were conducted at 150(2) K. The intensity data were integrated with the Bruker APEX2 software.[19] Absorption correction and scaling was performed with SADABS.[20] The structures were solved with SHELXS-97.[21] Least-squares refinement was performed with SHELXL-2013[19] against F^2 of all reflections. All non-hydrogen atoms were refined with anisotropic displacement parameters. Hydrogen atoms were located at calculated positions using a riding model. Details of the X-ray crystal structures are listed in the SI (Table S1).

Computational Methods. Density functional theory (DFT) calculations were carried out with the Turbomole 6.5 program package[22] using the BP86[23] functional with def2-TZVP[24] basis sets and resolution of identity[25] approximation. Vibrational analysis of calculated stationary points revealed no negative eigenvalues for minima and one negative eigenvalue for the transition state. The UV−vis transitions of complexes **A**, **B**, and **C** were calculated with TD-DFT (nroots = 50; maxdim = 600; triplets = false) as implemented in the ORCA package[26] at the b3-lyp[27] level (RIJCOSX[28]) using the def2-TZVP basis set. ZORA[29] scalar relativistic Hamiltonians (SpecialGridAtoms = 27, SpecialGridIntAcc = 7) and COSMO[30] dielectric solvent corrections (ε = 8.93; CH_2Cl_2) were included. The coordinates from the structures optimized in Turbomole were used as input for these ORCA TD-DFT calculations.

■ ASSOCIATED CONTENT

Supporting Information

The Supporting Information is available free of charge on the ACS Publications website at DOI: 10.1021/acs.organomet.5b00644.

DFT structures, TD-DFT calculations, UV−vis spectra, and kinetic curves (PDF)
Crystallographic data (CIF)
Crystallographic data (CIF)
Molecular structure (XYZ)

■ AUTHOR INFORMATION

Corresponding Author

*E-mail: w.i.dzik@uva.nl.

Notes

The authors declare no competing financial interest.

■ ACKNOWLEDGMENTS

We thank the NRSC-C and The Netherlands Organization for Scientific Research (NWO-CW, VENI grant 722.013.002) for funding. Helpful assistance from Fei Wu and Tatu Kumpulainen (Molecular Photonics, University of Amsterdam) with mathematics and global fit is acknowledged.

■ REFERENCES

(1) Feringa, B. L. *Molecular Switches*; VCH: New York, 2001.

(2) (a) Ceroni, P.; Credi, A.; Venturi, M. *Chem. Soc. Rev.* **2014**, *43*, 4068−4083. (b) Sato, O.; Cui, A.; Matsuda, R.; Tao, J.; Hayami, S. *Acc. Chem. Res.* **2007**, *40*, 361−369. (c) Bianchi, A.; Delgado-Pinar, E.; García-España, E.; Giorgi, C.; Pina, F. *Coord. Chem. Rev.* **2014**, *260*, 156−215. (d) Harvey, E. C.; Feringa, B. L.; Vos, J. G.; Browne, W. R.; Pryce, M. T. *Coord. Chem. Rev.* **2015**, *282*−*283*, 77−86. (e) Beharry, A. A.; Woolley, G. A. *Chem. Soc. Rev.* **2011**, *40*, 4422−4437.

(3) (a) Roux, C.; Zarembowitch, J.; Gallois, B.; Granier, T.; Claude, R. *Inorg. Chem.* **1994**, *33*, 2273−2279. (b) Boillot, M.-L; Roux, C.; Audiére, J.-P.; Dausse, A.; Zarembowitch, J. *Inorg. Chem.* **1996**, *35*, 3975−3980. (c) Hasegawa, Y.; Takahashi, K.; Kume, S.; Nishihara, H. *Chem. Commun.* **2011**, *47*, 6846−6848. (d) Venkataramani, S.; Jana, U.; Dommaschk, M.; Sönnichsen, D.; Tuczek, F.; Herges, R. *Science* **2011**, *331*, 445−448. (e) Thies, S.; Sell, H.; Schütt, C.; Bornholdt, C.; Näther, C.; Tuczek, F.; Herges, R. *J. Am. Chem. Soc.* **2011**, *133*, 16243−16250.

(4) (a) Kojima, T.; Morimoto, T.; Sakamoto, T.; Miyazaki, S.; Fukuzumi, S. *Chem. - Eur. J.* **2008**, *14*, 8904−8915. (b) Weisser, F.; Hohloch, S.; Plebst, S.; Schweinfurth, D.; Sarkar, B. *Chem. - Eur. J.* **2014**, *20*, 781−793. (c) Weisser, F.; Plebst, S.; Hohloch, S.; van der Meer, M.; Manck, S.; Führer, F.; Radtke, V.; Leichnitz, D.; Sarkar, B. *Inorg. Chem.* **2015**, *54*, 4621−4635.

DOI: 10.1021/acs.organomet.5b00644
Organometallics XXXX, XXX, XXX−XXX

(5) (a) Shaw, B.; Ike, U. U.; Perera, S. D.; Thornton-Pett. *Inorg. Chim. Acta* **1998**, *279*, 95−103. (b) Doux, M.; Mézailles, N.; Ricard, L.; Le Floch, P.; Vaz, P. D.; Calhorda, M. J.; Mahabiersing, T.; Hartl, F. *Inorg. Chem.* **2005**, *44*, 9213−9224. (c) Harkins, S. B.; Peters, J. C. *Inorg. Chem.* **2006**, *45*, 4316−4318.

(6) (a) Kluwer, A. M.; Kapre, R.; Hartl, F.; Lutz, M.; Spek, A. L.; Brouwer, A. M.; van Leeuwen, P. W. N. M.; Reek, J. N. H. *Proc. Natl. Acad. Sci. U. S. A.* **2009**, *106*, 10460−10465. (b) Derossi, S.; Becker, R.; Li, P.; Hartl, F.; Reek, J. N. H. *Dalton Trans.* **2014**, *43*, 8363−8367. (c) Li, P.; Amirjalayer, S.; Hartl, F.; Lutz, M.; de Bruin, B.; Becker, R.; Woutersen, S.; Reek, J. N. H. *Inorg. Chem.* **2014**, *53*, 5373−5383. (d) Nasalevich, M. A.; Becker, R.; Ramos-Fernandez, E. V.; Castellanos, S.; Veber, S. L.; Fedin, M. V.; Kapteijn, F.; Reek, J. N. H.; van der Vlugt, J. I.; Gascon, J. *Energy Environ. Sci.* **2015**, *8*, 364−375. (e) Li, P.; Zaffaroni, R.; de Bruin, B.; Reek, J. N. H. *Chem. - Eur. J.* **2015**, *21*, 4027−4038.

(7) A related well-defined mononuclear iron complex with tris(2-(diphenylphosphino)phenyl)phosphine—a tetradentate derivative of the TP ligand—has been recently developed as a homogeneous catalyst for hydrogenation reactions. See: (a) Ziebart, C.; Federsel, C.; Anbarasan, P.; Jackstell, R.; Baumann, R.; Spannenberg, A.; Beller, M. *J. Am. Chem. Soc.* **2012**, *134*, 20701−20704. (b) Wienhöfer, G.; Westerhaus, F. A.; Junge, K.; Ludwig, R.; Beller, M. *Chem. - Eur. J.* **2013**, *19*, 7701−7707.

(8) (a) Hartley, J. G.; Venanzi, L. M.; Goodall, D. C. *J. Chem. Soc.* **1963**, 3930−3936. (b) Chiswell, B.; Venanzi, L. M. *J. Chem. Soc. A* **1966**, 417−419. (c) Bigoli, F.; Curreli, S.; Deplano, P.; Leoni, L.; Mercuri, M. L.; Pellinghelli, M. A.; Serpe, A.; Trogu, E. F. *J. Chem. Soc., Dalton Trans.* **2002**, 1985−1991. (d) Nickl, C.; Eichele, K.; Wesemann, L. *Dalton Trans.* **2012**, *41*, 243−250. (e) Zank, J.; Schier, A.; Schmidbaur, H. *J. Chem. Soc., Dalton Trans.* **1998**, 323−324. (f) Sigl, M.; Schier, A.; Schmidbaur, H. *Eur. J. Inorg. Chem.* **1998**, *1998*, 203−210. (g) Zank, J.; Schier, A.; Schmidbaur, H. *J. Chem. Soc., Dalton Trans.* **1999**, 415−420. (h) Zank, J.; Schier, A.; Schmidbaur, H. *J. Chem. Soc., Dalton Trans.* **1999**, 415−420. (i) Chakkaradhari, G.; Belyaev, A. A.; Karttunen, A. J.; Sivchik, V.; Tunik, S. P.; Koshevoy, I. O. *Dalton Trans.* **2015**, *44*, 13294−13304.

(9) For some recent examples: (a) Pan, B.; Evers-McGregor, D. A.; Bezpalko, W. W.; Foxman, B. M.; Thomas, C. M. *Inorg. Chem.* **2013**, *52*, 9583−9589. (b) Ray, M. J.; Randall, R. A. M.; Athukorala Archchige, K. S.; Slawin, A. M. Z.; Bühl, M.; Lebl, T.; Kilian, P. *Inorg. Chem.* **2013**, *52*, 4346−4359. (c) Mazzeo, M.; Strianese, M.; Kühl, O.; Peters, J. C. *Dalton Trans.* **2011**, *40*, 9026−9033. (d) Bauer, R. C.; Gloaguen, Y.; Lutz, M.; Reek, J. N. H.; de Bruin, B.; van der Vlugt, J. I. *Dalton Trans.* **2011**, *40*, 8822−8829. (e) Mazzeo, M.; Lamberti, M.; Massa, A.; Scettri, A.; Pellecchia, C.; Peters, J. C. *Organometallics* **2008**, *27*, 5741−5743. (f) Goikhman, R.; Aizenberg, M.; Ben-David, Y.; Shimon, L. J. W.; Milstein, D. *Organometallics* **2002**, *21*, 5060−5065. (g) Beck, C. M.; Rathmill, S. E.; Park, Y. J.; Chen, J.; Crabtree, R. H. *Organometallics* **1999**, *18*, 5311−5317.

(10) (a) Bellachioma, G.; Cardaci, G.; Macchioni, A.; Venturi, C.; Zuccaccia, C. *J. Organomet. Chem.* **2006**, *691*, 3881−3888. (b) Rath, N. P.; Stouffer, M.; Janssen, M. K.; Bleeke, J. R. *Acta Crystallogr., Sect. E: Struct. Rep. Online* **2011**, *E67*, m462.

(11) (a) Johnson, B. F. G.; Lewis, L.; Robinson, P. W.; Miller, R. *J. Chem. Soc. A* **1968**, 1043−1048. (b) Pańkowski, M.; Bigorgne, M. *J. Organomet. Chem.* **1969**, *19*, 393−398. (c) Pańkowski, M.; Bigorgne, M. *J. Organomet. Chem.* **1977**, *125*, 231−252.

(12) (a) Bitterwolf, T. E. *J. Organomet. Chem.* **2008**, *693*, 2091−2096. (b) Bitterwolf, T. E.; Thornley, W.; Crawford, J. L. *Inorg. Chim. Acta* **2008**, *361*, 3271−3282.

(13) Irradiation of **A** with a 405 nm LED light led to a transient, NMR-silent species which re-formed species **A** within 2 h.

(14) Formation of species **D** and **E** was not observed experimentally. Formation of **D** would require dissociation of the central PPh-donor combined with pyramidal inversion at its P atom, which likely has a high energy barrier. We speculate that the fact that **E** does not form has a steric reason; recoordination of Cl to the (photogenerated) five-coordinated intermediate to form **E** is hindered by the Ph group of the central P-donor in a *mer*-coordination mode (see the SI, Scheme S3).

(15) (a) Jana, B.; Ellern, A.; Pestovsky, O.; Sadow, A.; Bakac, A. *Inorg. Chem.* **2011**, *50*, 3010−3016. (b) Sato, S.; Matubara, Y.; Koike, K.; Falkenström, M.; Katayama, T.; Ishibashi, Y.; Miyasaka, H.; Taniguchi, S.; Chosrowjan, H.; Mataga, N.; Koshihara, S.; Onda, K.; Ishitani, O. *Chem. - Eur. J.* **2012**, *18*, 15722−15734.

(16) Kleverlaan, C. J.; Hartl, F.; Stufkens, D. J. *J. Organomet. Chem.* **1998**, *561*, 57−65.

(17) A C_s symmetric transient species was observed that fully decayed within 1 h after mixing. ^{31}P NMR: δ 108.88 (t, J = 31.2 Hz), 63.33 (d, J = 31.0 Hz).

(18) (a) Mialocq, J. C.; Armand, X.; Marguet, S. *J. Photochem. Photobiol., A* **1993**, *69*, 351−356. (b) Kuhn, H. J.; Braslavsky, S. E.; Schmidt, R. *Pure Appl. Chem.* **2004**, *76*, 2105−2146.

(19) *APEX2* software; Bruker: Madison, WI, USA, 2014. Weigend, F.; Ahlrichs, R. *Phys. Chem. Chem. Phys.* **2005**, *7*, 3297−3305.

(20) *SAINT*, version 6.02, and *SADABS*, version 2.03; Bruker AXS, Inc.: Madison, WI, 2002.

(21) Sheldrick, G. M. *Acta Crystallogr., Sect. A: Found. Crystallogr.* **2008**, *A64*, 112−122.

(22) Ahlrichs, R.; Bär, M.; Barton, H.-P.; Bauernschmitt, R.; Böcher, S.; Rhrig, M.; Eichkorn, K.; Elliott, S.; Furche, F.; Haase, F.; M. Häser, C. Hättig, Horn, H.; Huber, C.; Huniar, U.; Kattannek, M.; A. Köhn, C. Kölmel, Kollwitz, M.; May, K.; Ochsenfeld, C.; Öhm, H.; Schäfer, A.; Schneider, U.; Treutler, O.; Tsereteli, K.; Unterreiner, B.; von Arnim, M.; Weigend, F.; Weis, P.; Weiss, H. *Turbomole* Version 6.4; Theoretical Chemistry Group, University of Karlsruhe: Karlruhe, Germany, January 2002.

(23) (a) Becke, A. D. *Phys. Rev. A: At., Mol., Opt. Phys.* **1988**, *38*, 3098−3110. (b) Perdew, J. P. *Phys. Rev. B: Condens. Matter Mater. Phys.* **1986**, *33*, 8822−8824. (c) Perdew, J. P. *Phys. Rev. B: Condens. Matter Mater. Phys.* **1986**, *34*, 7406−7406.

(24) Weigend, F.; Ahlrichs, R. *Phys. Chem. Chem. Phys.* **2005**, *7*, 3297−3305.

(25) Sierka, M.; Hogekamp, A.; Ahlrichs, R. *J. Chem. Phys.* **2003**, *118*, 9136−9148.

(26) Neese, F. *ORCA−an ab Initio, Density Functional and Semiempirical Program Package*, version 3.0.2; Max-Planck-Institut für Bioanorganische Chemie: Mülheim an der Ruhr, 2009.

(27) (a) Lee, C.; Yang, W.; Parr, R. G. *Phys. Rev. B: Condens. Matter Mater. Phys.* **1988**, *37*, 785−789. (b) Becke, A. D. *J. Chem. Phys.* **1993**, *98*, 1372−1377. (c) Becke, A. D. *J. Chem. Phys.* **1993**, *98*, 5648−5652. (d) Calculations were performed using the Turbomole functional b3-lyp, which is not fully identical to the Gaussian B3LYP functional.

(28) Neese, F.; Wennmohs, F.; Hansen, A.; Becker, U. *Chem. Phys.* **2009**, *356*, 98−109.

(29) (a) van Lenthe, E.; Baerends, E. J.; Snijders, J. G. *J. Chem. Phys.* **1993**, *99*, 4597−4610. (b) van Wüllen, C. *J. Chem. Phys.* **1998**, *109*, 392−399.

(30) Klamt, A.; Schüürmann, G. *J. Chem. Soc., Perkin Trans. 2* **1993**, *2*, 799−805.

DOI: 10.1021/acs.organomet.5b00644
Organometallics XXXX, XXX, XXX−XXX